Chemical, Electrochemical, Gravimetric, and Microscopic Studies on Antimicrobial Silver Films

Fu-Ren F. Fan and Allen J. Bard*

Department of Chemistry and Biochemistry, University of Texas at Austin, Austin, Texas 78712

Received: July 5, 2001; In Final Form: October 30, 2001

Silver compounds are of interest because of their antimicrobial and other biological activity. Electrochemical and chemical (e.g., dissolution) properties of silver films of various origins, e.g., sputtered Acticoat antimicrobial silver samples, electrodeposited Ag metal and electrooxidized silver samples in various media have been studied with electrochemical techniques, quartz crystal microbalance (QCM) gravimetry, X-ray diffraction, atomic force microscopy (AFM), and scanning electrochemical microscopy (SECM). Examination of several sputtered antimicrobial silver samples with AFM reveals their nanometer grainy aggregate structures. The electrochemical results suggest that the sputtered antimicrobial films contain both Ag(0) and Ag(I) (in the form of Ag_2O, AgOH, or a mixture of these). While the dissolution of metallic Ag or antimicrobial films that were completely reduced to the Ag(0) form is small in aqueous 1.0 M $NaClO_4$ solution, films containing Ag(I) are soluble. The initial dissolution rate of an antimicrobial film in 1.0 M $NaClO_4$ under open-circuit conditions was estimated to be about 3.6 $(\mu g/h)/cm^2$ in an unstirred condition. The SECM/QCM results suggest that the dissolved silver species contains both Ag(I) and Ag(0), with diffusion coefficients in the range $(3.5-4.0) \times 10^{-6}$ cm^2/s. Small clusters containing Ag(0) and Ag(I) (as well as O and H) are proposed for these dissolved silver species.

Introduction

Silver compounds have been exploited for their medicinal properties for centuries.[1] Gibbard first systematically investigated the antimicrobial activity of silver.[2] He found that if silver is cleaned mechanically with abrasive coated cloth or paper, it becomes inactive. If molten silver is allowed to cool in an atmosphere of hydrogen, no activity was found. However, when the cooling of molten silver was carried out in air, antimicrobial activity was observed. Similar results were found when silver metal was treated with nitric acid, resulting in the dissolution of silver metal and the formation of an oxide surface layer. Today, silver sulfadiazine is an important topical treatment for burn wounds[3] and silver nitrate is still used as a prophylaxis in neonatal opthalmia.[4] Another remarkable and potentially useful effect is the electrical silver antisepsis, in which a sustained antibacterial environment is produced near a metallic silver anode with low-level electrical currents.[5] The dynamics of formation of zones of inhibition in semisolid media is still not well understood. The generation of diffusable and ionized silver species at the electrode surface and their diffusion coefficients were proposed to be important factors but these were never determined. The special antimicrobial property of silver, as reported, is quite metal-specific and efficient.

Recently, layers of silver produced by sputtering under different conditions to produce nanoparticles of silver species have been produced and studied. Such films, called Acticoat films (Westaim Biomedical Corp., Fort Saskatchewan, Alberta), have been shown to have significantly higher bactericidal properties than simple Ag^+ solutions. On the basis of Acél's hypothesis[6] that Ag^+ ions are responsible for the antimicrobial activity of silver, Djokic and Burrell[7] have recently correlated the open-circuit potential vs time behavior of a silver film under physiological solutions to its antimicrobial effect. They found

that only silver films containing silver oxides showed a decrease in the open-circuit potential vs time curves and enhanced antimicrobial activity. Changes in the open-circuit potential were not found when pure metallic silver was exposed to physiological solutions and no antimicrobial activity was observed. More recently, Olson et al.[8] showed that Acticoat dressings increase wound healing rates in addition to demonstrating good antimicrobial activity.

An important issue with these materials is the nature of the soluble silver species that form and produce the enhanced biological responses. We studied the electrochemical and chemical (e.g., dissolution) properties of silver films of various types, e.g., sputtered Acticoat antimicrobial silver samples (supplied by Westaim), metallurgical, electrodeposited and electrooxidized silver samples in various media. Several different techniques, including X-ray diffraction (XRD), electrochemistry (EC), scanning electrochemical microscopy (SECM), quartz crystal microbalance (QCM) gravimetry, and optical and atomic force microscopy (AFM) were used to investigate these films. In this report, we focus on the EC behavior and dissolution processes of the sputtered antimicrobial silver samples in different media and compare these results with those with electrodeposited films.

Experimental Section

Chemicals. All chemicals were of reagent grade and were used without further purification. All aqueous solutions were prepared from Millipore reagent water (>18 MΩ). A silver disk electrode was prepared from a 0.5 mm diameter silver wire (99.9%) (Aldrich Chemical Co., Milwaukee, WI) by sealing it in ULTRA-MOUNT (Buehler, Lake Bluff, IL). The sealed end was polished with sandpaper until the wire cross section was exposed. The disk electrode was then polished successively with

1- and 0.25-μm diamond paste and finally with 0.05-μm alumina. Electrodeposition of silver was performed on Au substrates from 1 M NaClO$_4$ solution containing 1 or 5 mM AgNO$_3$. A NaClO$_4$ solution was used as the supporting electrolyte to adjust the ionic strength of the solution to 1.0 M. If not otherwise mentioned, all experiments were carried out in the ambient environment and the solution was not intentionally deaerated.

Antimicrobial Films. These films were prepared by sputtering of silver metal in a controlled atmosphere. Those called "base coat" (BC) films were produced in a nitrogen atmosphere containing 2% oxygen. Those called "optical interference layer" (IL) films were produced under the same conditions with an atmosphere containing 4% oxygen.

Techniques and Apparatus. Electrochemical measurements were carried out on a PAR 173 potentiostat/galvanostat equipped with a PAR 179 digital coulometer and a PAR 175 universal programmer (Princeton Applied Research, Princeton, NJ) or on a custom-built bipotentiostat.

We applied an O-ring seal to the sputtered samples to form an active area of ca. 0.5 cm^2. A silver wire was used as the quasireference electrode (AgQRE), whose potential was calibrated with respect to a saturated sodium chloride calomel reference electrode (SSCE).

The SECM instrument used in this work was either a custom-built unit, which has been described previously,[9] or a CH Instruments (Austin, TX) Model 900 SECM. A 10- or 25-μm diameter Pt disk-in-glass microelectrode was used as the tip in SECM and was constructed on the basis of the procedures described previously.[10] X-ray diffraction was carried out on an XRD (Philips APD 3520/PW 1729 X-ray generator), and AFM images were taken with a Nanoscope III scanning probe microscope (SPM) (Digital Instruments, Santa Barbara, CA). The QCM instrument used here has been described previously.[11] The 5-MHz QCM crystals (Maxtek, Torrance, CA) were patterned with a 0.5-in.-diameter gold electrode on one side and a 0.25-in.-diameter electrode on the other. The silver films were physically vapor-deposited or electrodeposited on the side with the smaller active area. The QCM data in most cases are presented in terms of the frequency change (Δf in Hz). The frequency change was converted to the mass change (ΔM) on the basis of[12]

$$\Delta f = -C_f \Delta M + \Delta f_0 \qquad (1)$$

where C_f, the sensitivity constant, is determined experimentally for a given constant active area, A, of the QCM crystal, and Δf_0 is a constant related to the density and viscosity of the medium and is determined experimentally.

Results and Discussions

I. Observations by Optical and Atomic Force Microscopies. We have carried out microscopic examination of several sputtered silver samples with AFM and optical microscopes. A typical AFM image of the IL of a fresh sputtered antimicrobial silver sample shows a uniformly distributed submicron grainy aggregate structure (not shown). The smallest grains revealed by AFM are on the order of $10-20$ nm. As compared with an IL film, an antimicrobial BC shows a substantially larger grain size (on the order of $50-150$ nm).

II. Electrochemical Measurements. If not otherwise mentioned, voltammetric and coulometric experiments[13] were carried out in a solution containing 1.0 M NaClO$_4$ as the supporting
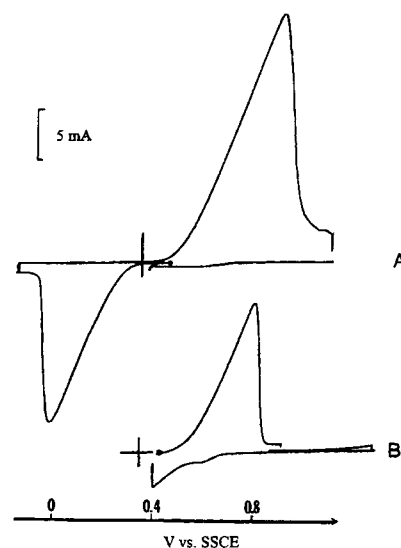
Figure 1. (A) Voltammetric curve of a fresh sputtered antimicrobial silver film (BC) in 1.0 M NaClO$_4$ solution. The electrode potential is scanned toward negative potentials first from the rest potential. (B) Voltammetric curve of a fresh sputtered silver sample (BC) in 1.0 M NaClO$_4$ solution. The electrode potential is scanned toward positive potentials first from the rest potential. The electroactive area of the sample is 0.5 cm^2. The potential scan rate is 0.1 V/s.

TABLE 1: Coulometric Measurements[a]

sample	type	Q_c, C	Q_a, C	$|Q_a/Q_c|$
5652[b]	BC	-4.9×10^{-2}	1.01×10^{-1}	2.06
5652[c]	BC	-4.7×10^{-2}	1.10×10^{-1}	2.34
5652[d]	BC	-5.0×10^{-2}	9.4×10^{-2}	1.89
5652[e]	BC	-4.2×10^{-2}	9.5×10^{-2}	2.26
5652[f]	BC	-5.0×10^{-2}	1.06×10^{-1}	2.12
5660	IL	-2.18×10^{-2}	2.0×10^{-2}	0.92
5660	IL	-2.40×10^{-2}	2.0×10^{-2}	0.83
5661	IL	-4.0×10^{-2}	3.93×10^{-2}	0.98
5662	IL	-8.8×10^{-2}	7.0×10^{-2}	0.80
5662	IL	-1.2×10^{-1}	1.0×10^{-1}	0.83

[a] If not otherwise mentioned, the measurements were carried out in air-saturated 1.0 M NaClO$_4$ solution. [b] Sample after used in XRD experiment. [c] Same sample as used in b, but EC measurement at different location. [d] New #5652 sample. [e] New #5652 sample. [f] This experiment was carried out in deaerated 1.0 M NaClO$_4$ solution.

electrolyte and the solution was not deaerated or buffered (pH about 6.5). Figure 1A shows the voltammetric curve of a sputtered silver BC sample (300 nm thick with no IL), which had a rest potential near 0.42 V vs SSCE in 1.0 M NaClO$_4$. The electrode potential was first scanned toward negative potentials from the rest potential to the cathodic limit. After holding the potential there to collect the total amount of charge, Q_c, corresponding to the reduction of all of the reducible silver species (e.g., Ag(I), Ag(II), ...), the electrode potential was then scanned toward positive potentials to the anodic limit where Ag(0) was oxidized. At this potential, the total amount of charge, Q_a, corresponded to the oxidation of oxidizable silver species originally present in the sample and those generated in the cathodization process. As measured, $Q_c = -4.9 \times 10^{-2}$ C and $Q_a = 1.01 \times 10^{-1}$ C and thus $|Q_a/Q_c| = 2.06$. If one scanned a fresh sample directly from its rest potential to the same anodic limit at which Q_a was measured, a value of 5.6×10^{-2} C was obtained (see Figure 1B). Note that on a bare Au film (on glass cover slip), negligible EC activity and charge was found over a similar anodic potential range. We summarize the results for several samples in Table 1. As shown, the measured $|Q_a/Q_c|$ values for these BC samples are slightly higher than 2,

Antimicrobial Silver Films

J. Phys. Chem. B, Vol. 106, No. 2, 2002 **281**

suggesting that they contain slightly more than 50% of Ag(0) and somewhat less than 50% of oxidized silver species. The Q_a/Q_c varied somewhat from sample to sample. Note that very similar EC behavior was observed for a BC sample in a deaerated 1.0 M $NaClO_4$ solution, indicating that the reduction peak near 0 V is not associated with dissolved oxygen or its reaction product (if any) with the silver sample after immersing it in the electrolyte. However, we cannot exclude the possibility that the reduction peak near 0 V is associated with a reaction product between water, H^+ or OH^-, and the sputtered silver sample based on this experiment.

A sputtered IL silver sample (160 nm thick and no silver BC) has a substantially higher rest potential (about 0.71 V vs SSCE) as compared to a BC sample. The measured Q_c at -0.177 V vs SSCE where the reduction of the reducible silver species takes place is -4.0×10^{-2} C and Q_a at 0.845 V, where the Ag(0) species generated is reoxidized, is 3.93×10^{-2} C. Hence, $|Q_a/Q_c| = 0.98$. Note that there is no appreciable EC activity taking place at a fresh IL (160 nm) sample at a bias of 0.84 V vs SSCE, indicating that no appreciable Ag(0) species is initially present in the sample. As summarized in Table 1, the measured values of $|Q_a/Q_c|$ for all of the IL film samples (no BC) are only slightly lower than 1, suggesting that they initially contain Ag(I) as the predominant species and probably do not contain higher oxidation-state silver species, like Ag(II).

To see whether the reduction peak near 0 V vs SSCE observed on sputtered antimicrobial silver samples (BC or IL) was associated with the reduction of Ag(I) oxides, we grew a silver(I) oxide film on a silver disk (0.5-mm diameter) at 0.50 V vs SSCE in 0.1 M NaOH and 0.9 M $NaClO_4$ solution.[14] The oxide-covered silver electrode was rinsed with water and then immersed in a solution containing 1.0 M $NaClO_4$ for voltammetric measurement. As shown in Figure 2A, an oxide-covered Ag electrode has a rest potential near 0.35 V vs SSCE in 1.0 M $NaClO_4$, which is close to that of a sputtered BC sample. Scanning the electrode potential toward negative potentials from the rest potential produces a reduction peak near 0 V vs SSCE. The reduction peak nearly disappeared in subsequent cyclic scans between -0.25 and 0.35 V vs SSCE. In a different experiment, we carried out cyclic voltammetry to a more positive potential in 1.0 M $NaClO_4$ with a newly prepared oxide-covered silver disk electrode. As shown in Figure 2B, in addition to the cathodic peak (near 0 V vs SSCE) due to the reduction of Ag(I) oxide, we also observed the normal Ag^0 stripping and rereduction peak of Ag(I) taking place at more positive potentials (near 0.50 V vs SSCE). For comparison, the normal Ag^0 stripping and rereduction of Ag(I) on a freshly polished silver disk electrode is shown in Figure 2C. Note also that no reduction peak was observed near 0 V in 1.0 M $NaClO_4$ solution on a freshly polished silver disk electrode when its potential was initially scanned toward negative potentials from the rest potential. These results suggest that the reducible silver species present in both silver BC and silver IL are predominantly in the Ag(I) state. Voltammetric measurement has also been carried out in basic media and will be discussed in the following sections on SECM and QCM.

III. Scanning Electrochemical Microscopy. *A. Sputtered Silver Films in Neutral Media.* A fresh sputtered silver sample (IL on a glass cover slip) was mounted in an SECM cell equipped with a Pt tip (diameter = 25 μm) positioned at a distance of ca. 0.5 mm away from the surface of the sample. To eliminate possible chemical reactions between the silver sample and redox mediator, the SECM positioning was carried out with an optical microscope. About 10 min after the
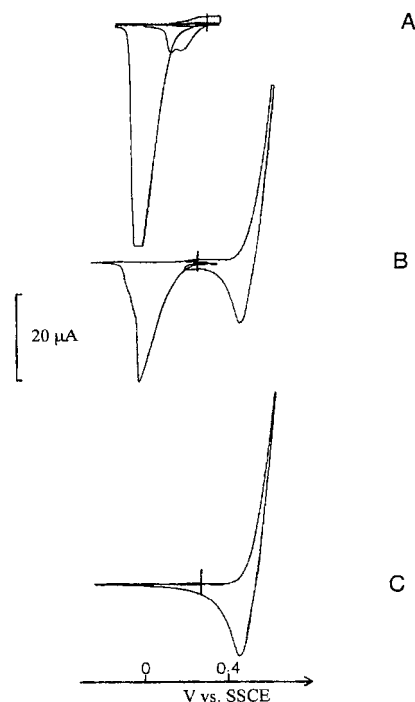

Figure 2. Voltammetric curves of an electrochemically grown silver oxide covered silver disk (diameter = 0.5 mm) in 1.0 M $NaClO_4$ solution. The anodic potential scan limit is 0.35 V (A) and 0.6 V (B) vs SSCE. The electrode potential is scanned toward negative potentials first from the rest potential. (C) Voltammetric curve of a freshly polished silver disk (diameter = 0.5 mm) in 1.0 M $NaClO_4$ solution. The electrode potential is scanned toward positive potentials first from the rest potential. The potential scan rate is 0.1 V/s.
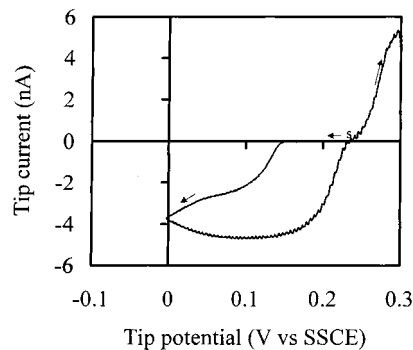
Figure 3. First tip cyclic voltammogram taken in 10 mM $NaClO_4$ solution. The tip (diameter = 25 μm) is positioned a few tenths of a millimeter away from a sputtered antimicrobial silver sample (IL on glass cover slip). The tip CV is taken after the silver substrate is immersed in the solution for ca. 10 min. The tip potential is scanned toward negative potentials first from the rest potential, while the antimicrobial silver sample is left at open-circuit condition. The tip potential scan rate is 10 mV/s.

introduction of a solution containing 10 mM $NaClO_4$ (pH 6) into the SECM cell, cyclic voltammetry on the tip, which detects any dissolved products from the film at open circuit, was carried out. In Figure 3, the first tip cyclic voltammogram (CV) is shown. As the tip potential was scanned in a negative direction from its rest potential (ca. 0.23 V vs SSCE), a significant cathodic current was observed near 0.15 V vs SSCE, which attained a quasi-steady-state value. Note that only a small background current was observed in this potential region when no silver sample was present. On the reverse scan, a higher reduction current was observed. This increase in reduction current is caused by the increase in the tip radius because of
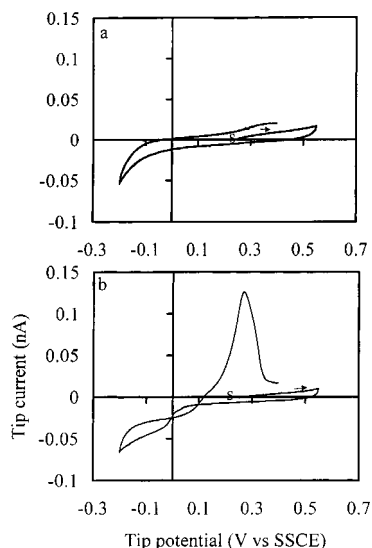
Figure 4. Two tip CV's at two different distances (curve a, $d = 2$ mm; curve b, $d = 0.2$ mm) from a sputtered antimicrobial silver BC immersed in 0.1 M NaOH and 0.9 M NaClO$_4$ for 40 min. Tip radius $= 5$ μm. The tip potential scan rate $= 10$ mV/s.

continued silver metal deposition. When the potential was scanned positive of ca. 0.2 V, substantial oxidation of the deposited Ag^0 took place. As shown in this figure, only part of the silver-stripping peak was recorded. Note that in the subsequent scans (ca. 6 min apart), the cathodic quasi-steady-state tip current continued to increase with time (not shown). This increase in the tip current is partly due to the growth of silver metal at the tip, as mentioned above and partly due to the increase in the concentration of reducible silver species dissolving from the sample. Quite differently, no appreciable *anodic* tip current was measured at potentials negative of 0.45 V vs SSCE when a freshly polished tip was scanned positive from its rest potential, indicating that no soluble Ag(0) species were detected in the solution for this IL sample.

On the basis of the results described above, we were unable to obtain a quantitative steady-state concentration profile of the soluble Ag(I) species in this medium, because the exact active area of the tip is time dependent from the fast continuous growth of silver metal on the tip. The time dependence of the dissolution process of the silver species also complicates the interpretation of the tip current vs distance profile. However, by slowing down the dissolution rate of the silver species in a dilute basic medium and by using other operation modes of SECM, e.g., the transient technique,[15] it is possible to estimate the diffusion coefficient and the instantaneous concentration profile of the soluble silver species as described below.

B. Silver Films in 0.1 M NaOH and 0.9 M NaClO$_4$. 1. Sputtered Silver Films. (a) Passive Dissolution. We show here that dissolution of a sputtered BC film in this medium produces both soluble Ag(I) and Ag(0) species whose concentrations and diffusion coefficients can be estimated by transient measurements at the tip. An unused sputtered BC silver sample was mounted in the SECM cell with a Pt tip (diameter $= 10$ μm) positioned close to the surface of the silver substrate. About 40 min after the introduction of a solution containing 0.1 M NaOH and 0.9 M NaClO$_4$ into the cell, a series of tip CV's were taken at different tip−substrate distances, d. Figure 4 shows two typical tip CVs taken at $d = 2$ and 0.2 mm, with the silver substrate left at open circuit. The tip potential was normally scanned positive from its rest potential to the anodic limit and then to the cathodic limit. After returning from the second anodic
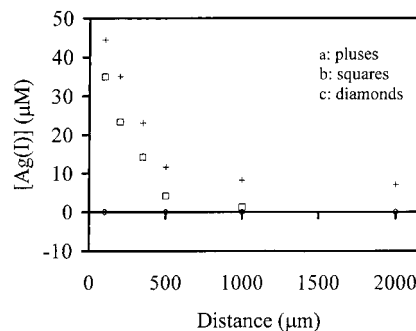
Figure 5. Distance dependence of the instantaneous concentration of the soluble Ag(I)-containing species near the surface of various silver substrates after immersion in 0.1 M NaOH and 0.9 M NaClO$_4$ for ca. 40−50 min. Curve a (pluses): a sputtered BC sample. Curve b (squares): an 80% oxidized electrochemically grown silver film. Curve c (diamonds): a fresh electrochemically grown silver metal film.

scan segment, the potential scan was stopped near the starting potential. As shown, in the reduction regime, a significantly larger reduction current is observed at smaller d and it reaches a quasi-steady-state value at potentials negative of 0.05 V vs SSCE. On the reverse scan to potentials positive of 0.15 V, one can observe several oxidation waves (or shoulders), which are similar, but not identical to those found with oxide films formed on bulk silver (see below). From the cathodic tip current plateau, one can estimate the concentration of the soluble reducible silver species from its diffusion coefficient (as determined by transient techniques discussed later) and the tip radius via eq 2 for the steady-state current at a disk microelectrode, $i_{D,ss}$.

$$i_{D,ss} = 4nFDCa \qquad (2)$$

where n is the number of electrons involved in the electrode reaction, F is the Faraday constant, a is the disk radius, C is the concentration, and D is the diffusion coefficient of the redox species. In the absence of complications, e.g., any substantial change in the electrode area due to the growth of silver metal on the tip, an approximate concentration profile can be obtained when $d \gg a$. Curve a of Figure 5 summarizes the estimated instantaneous concentration profiles of the total soluble Ag(I) species after a sputtered BC sample is immersed in 0.1 M NaOH and 0.9 M NaClO$_4$ for ca. 40 min. Although this profile shows only instantaneous rather than steady-state concentrations, the results clearly demonstrate that significant amounts of some reducible Ag(I)-containing species dissolves from the sample and diffuses as far as 1 mm away from the substrate in a time period of 40−50 min.

We employed a transient technique to determine the diffusion coefficient of the soluble redox species. The dissolution rate of the silver species from the sample in 0.1 M NaOH and 0.9 M NaClO$_4$ is slow compared to the time scale of the transient technique. Similarly, the reduction products at the tip are probably not highly soluble. Thus, in the transient experiment, where reduction of the Ag(I) species at the tip held near to the substrate occurs over a time of about 10 s, the silver substrate can be treated as an insulator. For SECM at an insulating substrate, its chronoamperometric response at short time scale can be approximated, within a constant, to that of a thin-layer cell (TLC) where the cavity is bounded by one electrode (the tip) and an insulating wall (the substrate). The SECM gap in this regime can be thought of as a "leaky" TLC and the transient tip current can be approximated by the following analytical expression:[16]

Antimicrobial Silver Films

J. Phys. Chem. B, Vol. 106, No. 2, 2002 **283**

$$i_T = i_{T,C} + (4nF\pi a^2 DC/d)\sum_{m=0}^{\infty}\exp[-(2m+1)^2\pi^2 Dt/d^2] \quad (3)$$

where $i_{T,C}$ accounts for the diffusion of the redox species to the tip from the space between the edges of the insulator surrounding the disk and the substrate. The simulated SECM transient for an insulating substrate[15] shows that one can obtain $i_{T,C}$ from the straight line portion of the plot of i_T vs $t^{-1/2}$ at long times, where $i_{T,C}$ is the instantaneous tip current when the current starts to deviate from the (i_T vs $t^{-1/2}$) line. As implied in eq 3, i_T can be expressed with reasonable accuracy (<2% error) in a single exponential form, when $t \geq 0.1d^2/D$ but shorter than the time when $i_{T,C}$ is determined. Note that eq 3 can be used to measure D without knowing C (if d is known) from the slope ($-\pi^2 D/d^2$) of the semilogarithmic plot of the tip current vs time. From the intercept, one can calculate the concentration C, if tip radius and n are known. Figure 6A shows a typical cathodic tip chronoamperometric curve at $d = 0.1$ mm when the tip potential was stepped from its rest potential (0.25 V vs SSCE) to -0.15 V. Figure 6B shows a semilogarithmic plot of the tip current (after correction for $i_{T,C}$) vs time, with a sputtered silver BC left at open circuit in the solution for 40 min. The plot shape conforms to eq 3 and provides a D value of ca. 4.0×10^{-6} cm^2/s for the soluble Ag(I)-containing species. This D value is 2−3 times smaller than the diffusion coefficients of Ag$^+$ determined from the polarography technique in neutral NaF or KNO$_3$ solution.[17] This smaller D value of the Ag(I)-containing species from film dissolution as compared to that of Ag$^+$ may reflect its cluster nature. We used this D value to estimate the total dissolved Ag(I) concentration at various distances from a sputtered silver BC on the basis of eq 2 (see curve a of Figure 5).

To determine the D value of the oxidizable [Ag(0)-containing] species, tip chronoamperometry at $d = 0.1$ mm was carried out with a fresh BC silver sample immersed in the solution at open circuit for ca. 40 min. Figure 7A shows a typical anodic tip chronoamperometric curve with the tip potential stepped from its rest potential to 0.45 V vs SSCE. Figure 7B shows the semilogarithmic plot of the tip current (after correction for $i_{T,C}$) vs time. A D value of 3.5×10^{-6} cm^2/s for the Ag(0)-containing species and a total Ag(0) concentration of ca. 0.7 mM can be calculated on the basis of the slope and the intercept of the semilog plot. Note that this estimated concentration is only an average instantaneous value, since the concentration of the redox species is not really uniformly distributed in the gap when the chronoamperometric measurement is carried out. A true steady-state concentration profile may still not be established in a time period of ca. 40 min.

(b) Electrochemically Induced Dissolution. We then studied the sputtered silver samples under potential control. Figure 8 shows the CV and Figure 9 illustrates the effect of the redox history (by potential cycling) of a sputtered antimicrobial BC sample on its dissolution behavior. With the tip left at open circuit, the potential of a silver substrate was scanned positive from its rest potential to the anodic limit and then to the cathodic limit (Figure 8). After cycling back to the starting potential from the second anodic scan segment, the substrate was left at open circuit. Curve a of Figure 9 shows the tip CV before the potential cycling of the silver substrate was carried out. With the tip positioned at $d = 0.1$ mm away from the silver substrate, only a small tip current was observed during the first anodic scan segment. After two oxidation−reduction cycles on the silver substrate, however, the tip detected a significant amount of oxidizable silver (presumably a Ag(0)-containing) species during
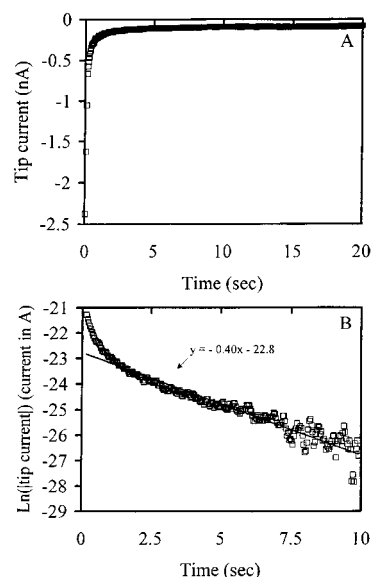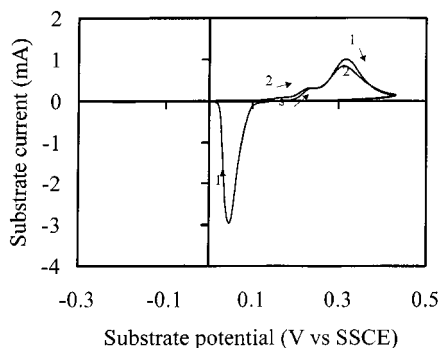

Figure 6. (A) Cathodic tip chronoamperometric curve at $d = 0.1$ mm away from a sputtered antimicrobial silver BC sample immersed in 0.1 M NaOH and 0.9 M NaClO$_4$ at an open circuit for ca. 40 min. The tip potential is stepped from $+0.25$ to -0.15 V vs SSCE. (B) shows the semilogarithmic plot of the tip current vs time after correction for $i_{T,C}$ based on eq 3.
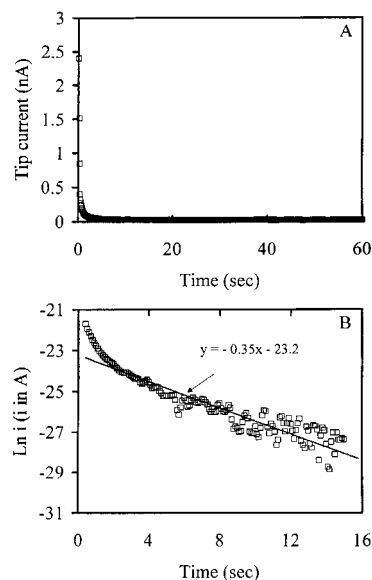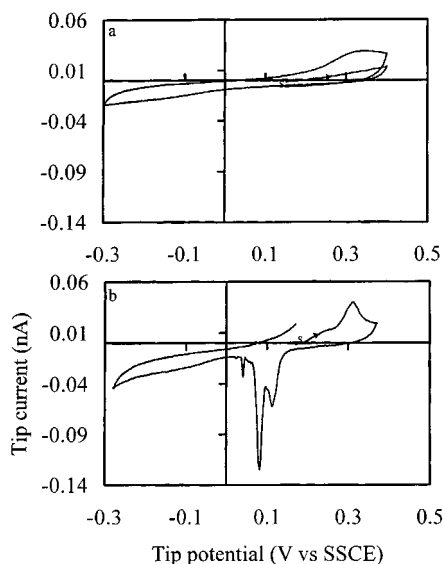

Figure 7. (A) Anodic tip chronoamperometric curve at $d = 0.1$ mm away from a sputtered antimicrobial silver BC sample immersed in 0.1 M NaOH and 0.9 M NaClO$_4$ at an open-circuit for ca. 40 min. The tip potential was stepped from 0.25 to 0.45 V g SSCE. (B) shows the semilogarithmic plot of the tip current (i) vs time (after correction for $i_{T,C}$) based on eq 3.

the first anodic scan segment (see curve b of Figure 9). In the reduction regime at potentials positive of ca. 0.0 V vs SSCE, several peaks (or shoulders) are also observed, partly due to the rereduction of the oxidized silver species. As also shown in this figure, at tip potentials negative of 0.0 V, we observe a reductive tip current, which can be attributed to the diffusion of the Ag(I)-containing species to the tip from the space outside the tip−substrate gap. For comparison, we have also carried out similar types of SECM experiments on electrochemically grown silver and Ag(I) oxide samples as described below.

2. Silver Metal Films. A silver metal film ($Q_c = -30$ mC) electrodeposited on a gold on glass (Au/glass) substrate was immersed in the 0.1 M NaOH and 0.9 M NaClO$_4$ electrolyte

Figure 8. CV of a sputtered silver BC in 0.1 M NaOH and 0.9 M NaClO$_4$. Potential scan rate = 10 mV/s. The numbers on the curve indicate the sequence of potential scan.


Figure 9. Tip CV at d = 0.1 mm away from a sputtered antimicrobial silver BC sample immersed in 0.1 M NaOH and 0.9 M NaClO$_4$ at open circuit. Curve a: before two oxidation−reduction cycles. Curve b: after two oxidation−reduction cycles as shown in Figure 8. The potential scan rate = 10 mV/s.

solution for ca. 40 min at open circuit before a series of tip CV's were recorded for the tip at different distances. No appreciable redox current associated with any silver species can be detected in the potential range studied at any distance, indicating that the dissolution rate of a pure silver metal film is very small (curve c in Figure 5).

3. Electrochemically Oxidized Silver Films. (a) Passive Dissolution. The silver metal film used in the previous section was partially oxidized in 0.1 M NaOH and 0.9 M NaClO$_4$ (ca. 80% in terms of the charge collected). After washing and replacing with a fresh 0.1 M NaOH and 0.9 M NaClO$_4$ solution, the oxidized silver sample was immersed in this solution for ca. 40−50 min before tip cyclic voltammetric measurements were carried out. As shown in curve b of Figure 10 for this 80% oxidized silver sample, the tip (positioned at d = 0.1 mm away from the substrate) can detect in the initial anodic scan the presence of a small amount of Ag(0)-containing species and, from the cathodic scan, a much larger amount of Ag(I)-containing species. For comparison, the tip CV recorded at a similar distance over a silver metal film, immersed in the solution for a similar period, is shown in curve a. The reduction tip current shows considerable distance dependency. Curve b of Figure 5 summarizes the instantaneous concentration profile of the Ag(I)-containing species estimated from the quasi-steady-
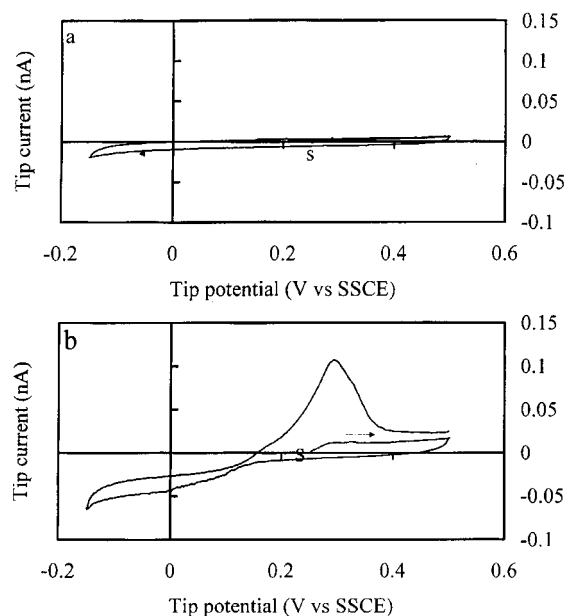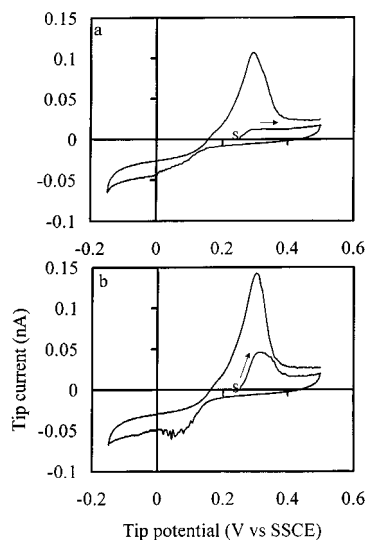

Figure 10. Tip CV with the tip positioned at d = 0.1 mm away from a fresh electrochemically grown silver metal film (curve a) immersed in 0.1 M NaOH and 0.9 M NaClO$_4$. Curve b: after ca. 80% of the silver is electrochemically oxidized. The tip potential scan rate = 10 mV/s.
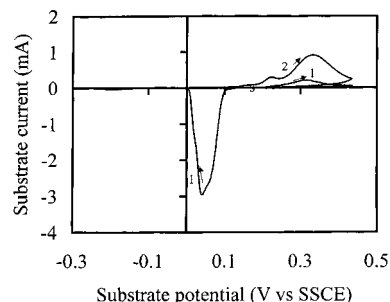
Figure 11. First CV of an 80% oxidized silver sample in 0.1 M NaOH and 0.9 M NaClO$_4$. The potential scan rate = 10 mV/s.

state reductive tip current and the diffusion coefficient ($D \cong 4.0 \times 10^{-6}$ cm^2/s) obtained from the chronoamperometric measurements.

(b) Electrochemically Induced Dissolution. Figure 11 shows the first CV of the 80% oxidized silver sample. As its potential was scanned positively from the rest potential, an oxidation peak was observed in the first anodic scan segment due to the oxidation of Ag(0) species remaining in the sample. In the remainder of the scan, one also observes several waves (or shoulders) more or less similar to those as described below. After the potential was scanned back to the starting potential, the silver substrate was left at open circuit and a tip CV was taken at d = 0.1 mm. An enhanced anodic tip current (compare curves a and b in Figure 12) was observed, indicating that more Ag(0)-containing species exists near the surface of the silver substrate after cycling the potential to positive values. The enhancement of the concentration of the Ag(0)-containing species (near the substrate surface) by potential cycling was apparently independent of the scan direction (anodic or cathodic) of the final scan segment, as long as the substrate was left at open circuit after redox cycling. However, the wave at the tip was strongly attenuated by biasing the substrate potential at either −0.15 V vs SSCE where the Ag(I)-containing species is reduced or at 0.5 V where the Ag(0)-containing species is oxidized (not shown). A bias of 0.5 V on the substrate will

Antimicrobial Silver Films

J. Phys. Chem. B, Vol. 106, No. 2, 2002 **285**

Figure 12. Tip CV with the tip positioned at $d = 0.1$ mm before (curve a) and after (curve b) the substrate has undergone the redox cycling as shown in Figure 11. The substrate is left at open circuit during cyclic voltammetric experiment.

deplete the Ag(0)-containing species near its surface. The decrease in the concentration of the Ag(0)-containing species by a bias of -0.15 V on the substrate might be associated with the low solubility of the silver metal film. These results also imply that the dissolution of the silver sample is facilitated by the coexistence of a Ag(I)/Ag(0) mixed-valence species interfaced with the electrolyte.

The formation of long-lived Ag(0)-containing species in a weak basic media described above confirms the results reported recently by ten Kortenaar et al.,[18] who found that nanometer-size silver clusters could be prepared by anodic dispersion of a silver electrode in aqueous NaOH solution free of stabilizing polymers. Nanometer-size silver particles or clusters are considered thermodynamically unstable in water, so that their preparation in aqueous solutions free of stabilizing polymers has remained a challenge.[19] Oxide encapsulation can improve the stability of silver clusters and also enhance their luminescent efficiency.[20] Other than these EC data, we have also found that the solubility of the sputtered silver samples strongly depended on the solution conditions. For example, a sputtered IL silver sample could dissolve nearly completely shortly after immersion in a solution containing 0.5 M acetic acid (HOAc) and 0.5 M sodium acetate (NaOAc). In the following section, we monitored the dissolution of sputtered silver samples (650 nm antimicrobial silver BC on a Au substrate) by EC quartz crystal microbalance (QCM) gravimetry and compared the results with those obtained for silver oxide films grown electrochemically.

IV. Electrochemical and Quartz Crystal Microbalance Measurements. *A. Electrochemical Deposition and Dissolution of Silver.* Both EC deposition and dissolution of silver metal at the QCM in a solution containing 1 mM AgNO$_3$ and 1.0 M NaClO$_4$ caused a 130 Hz change in the QCM frequency, Δf, for a charge, ΔQ, of 1 mC collected in either the deposition or stripping process. We thus determine the sensitivity of the QCM, C_f, as 0.117×10^9 Hz/g for a given active area, A, of the QCM crystal (eq 1). The equivalent weight of the deposit can be determined from the equation

$$\text{eq wt (g/eq)} = \frac{\Delta f / C_f}{\Delta Q / F} = \frac{0.825 \Delta f \,(\text{Hz})}{\Delta Q \,(\text{mC})} \quad (4)$$

where Δf is the frequency change with the passage of charge
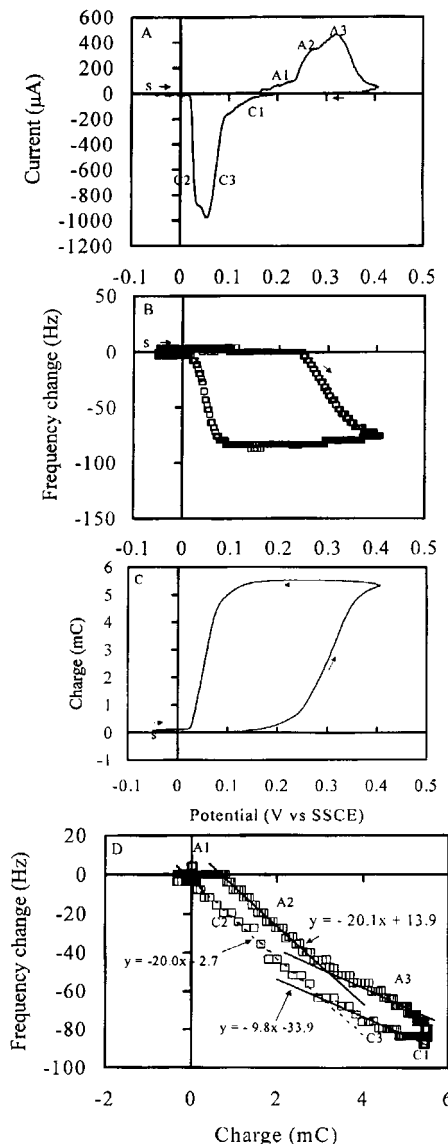
Figure 13. Voltammetric curve (A), frequency change vs potential curve (B), and charge vs potential curve (C) on an Ag-coated ($Q_c \sim 7$ mC) QCM in 0.1 M NaOH and 0.9 M NaClO$_4$ solution. Potential scan rate = 10 mV/s. The distinct oxidation and reduction waves are labeled on CV. D: Frequency change is plotted against the charge collected. The labeling on the curve is matched with that shown on A.

(mC), ΔQ; a small intercept of the (Δf vs ΔQ) curve is neglected. For a one-electron redox process, eq wt is the molecular weight of the compound deposited on or stripped from the QCM crystal. More detailed information for the calibration of the QCM is described in the Supporting Information section.

1. Oxide Formation on Silver in 0.1 M NaOH and 0.9 M NaClO$_4$. EC and QCM measurements were carried out to study the formation and removal of oxide films on silver films for comparison to those on antimicrobial films. As shown in curve A of Figure 13, when the potential of a freshly prepared silver-coated ($Q_c \sim 7$ mC) QCM sample was scanned positively from -0.066 V vs SSCE, at least three distinct anodic waves (A1, A2, and A3) were seen at potentials positive of 0.13 V. In the reverse scan, at least three distinct cathodic waves (C1, C2, and C3) at potentials negative of 0.13 V were found. The corresponding frequency change of the QCM and the charge collected are shown in curves B and C of the same figure. Clearly shown in these curves is that, during the appearance of A1 and C1, significant current flows, and charge is accumulated while the

frequency changes of the QCM are negligibly small. These small values of $|\Delta f/\Delta Q|$ might be associated with "the counteraction of the formation of soluble silver compound and phase formation" as proposed by Kautek et al.[21] They have also been assigned to the "charging or discharging," (i.e., adsorption and desorption)[22] of OH⁻ to or from the highly porous silver film. On the basis of the results discussed in the SECM section, we assign these negligibly small $|\Delta f/\Delta Q|$ values to EC processes involving soluble silver species in the vicinity of an oxidizing silver film in alkaline medium. As the potential is scanned positive to the second wave (A2), a significant decrease in the QCM frequency with an increase in the positive charge was observed. As shown in curve D, a $\Delta f/\Delta Q$ of -20.1 Hz/mC is calculated in this regime. This $\Delta f/\Delta Q$ value yields a Δ(eq wt) $= 17$, consistent with the formation of AgOH(s) based on the following EC reaction

$$Ag(s) + OH^- \rightarrow AgOH(s) + e \qquad (5)$$

where s denotes a solid phase. As the potential was scanned further to the third wave (A3), a $\Delta f/\Delta Q$ of -9.8 Hz/mC was obtained, corresponding to a mass gain of ca. 8 atomic units for the loss of one electron at the QCM. This result suggests the formation of Ag₂O(s) based on the overall reaction

$$2Ag(s) + 2\,OH^- \rightarrow Ag_2O(s) + H_2O + 2e \qquad (6)$$

Note that after scan reversal to wave C3, a $\Delta f/\Delta Q$ of -9.8 Hz/mC is found, corresponding to the reverse EC reaction of eq 6. In the potential region where wave C2 appears, a frequency increase of $\Delta f = 20$ Hz for a charge of $\Delta Q = -1$ mC passed indicates a mass loss of ca. 17 atomic units for the gain of one electron at the QCM. This result corresponds to the reverse EC reaction of eq 5.

2. QCM Measurements on Antimicrobial Silver Films in 1.0 M NaClO₄. The CV and the corresponding ΔQ and Δf responses of a fresh sputtered antimicrobial BC silver film coated on a quartz crystal for use in the QCM in a solution containing 1.0 M NaClO₄ are shown in Figure 14. As the potential of the silver film was scanned negative from its rest potential, a small reduction peak was observed near 0.1 V vs SSCE (curve A); this is attributed to the reduction of the Ag(I) species contained in the sample. Accompanying the current flow, the QCM frequency first decreased and then increased very slightly (observable on an expanded scale, not shown) while the magnitude of the negative charge collected in this regime increased monotonically (curve B). On the reverse scan, significant oxidation current flows (with the corresponding positive charge collection) started near 0.25 V vs SSCE and the positive charge appearing in the anodic peak was ca. 10 times that of the negative charges collected in the reduction regime (not shown). The $(\Delta f/\Delta Q)$ data shown in curve D indicate that there is some mass gain near the foot of the reduction peak, presumably due to the deposition of a silver metal from some Ag(I) species dissolved from the sample. At more negative potential, we obtain a $\Delta f/\Delta Q$ value of -13.1 Hz/mC, which is lower than the -9.6 Hz/mC expected for the reduction of Ag₂O(s) to Ag(s) but higher than the -20.5 Hz/mC for the reduction of AgOH(s) to Ag(s). We tentatively attribute this discrepancy to the existence of both types of Ag(I) oxide species: xAg₂O and yAgOH ($x{:}y \cong 1{:}1$). In the oxidation regime, a $\Delta f/\Delta Q$ value of ca. 145 Hz/mC is obtained. Considering that about a 10% mole fraction of the total silver exists in the Ag(I) oxide form, a $\Delta f/\Delta Q$ value of 145 Hz/mC is expected for the concurrent dissolution of these Ag(I) species
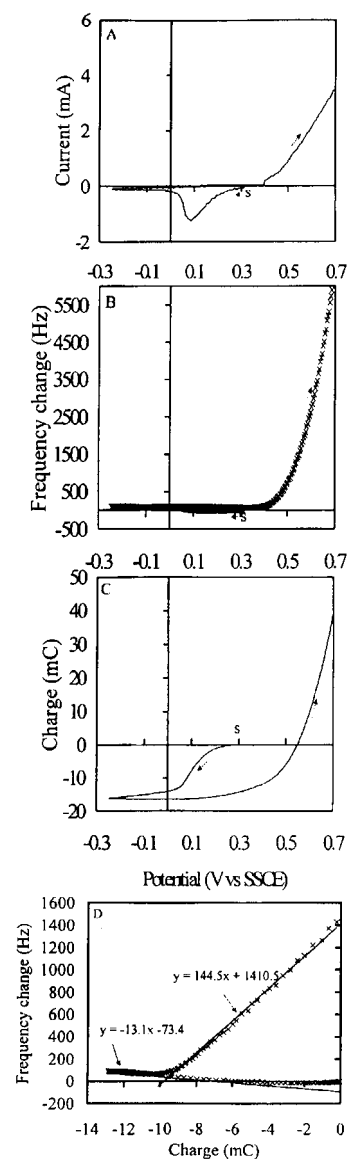
Figure 14. Voltammetric curve (A), frequency change vs potential curve (B), and charge vs potential curve (C) on a QCM coated with a sputtered antimicrobial BC silver film in 1.0 M NaClO₄ solution. Potential scan rate = 10 mV/s. D: Frequency change is plotted against charge collected.

together with the normal Ag(0) stripping ($\Delta f/\Delta Q = 130$ Hz/mC in 1.0 M NaClO₄) as discussed above.

B. Chemical Precipitation and Dissolution Processes of Silver. In Figure 15, we compare the weight loss in 1.0 M NaClO₄ as a function of time of sputtered samples (650 nm sputtered antimicrobial silver BC) (curves a–d) with that of an electrochemically grown silver oxide film (curve e) under different conditions. As shown in curve a, for a freshly sputtered sample (active area ca. 0.31 cm²), no appreciable weight change was observed in the air under ambient conditions over a 1-h period. However, the same sample immersed in 1.0 M NaClO₄ solution at open-circuit conditions showed considerable weight loss (ca. 1.2 μg) in 1 h (curve b). This weight loss was, however, only about one-fifth of that of an electrochemically grown silver oxide film ($Q_a = 9.0$ mC) of about the same area (curve e). The difference in the weight loss represents the different solubility for different samples prepared by different methods. As suggested from the EC and XRD results (some of the XRD data are shown in the Supporting Information section), we know

Antimicrobial Silver Films

J. Phys. Chem. B, Vol. 106, No. 2, 2002 **287**
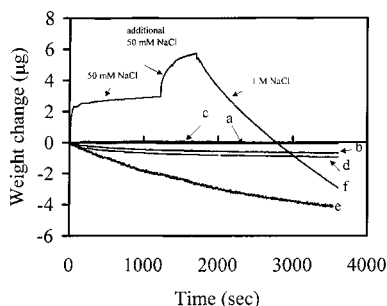
Figure 15. Passive dissolution of various silver samples in 1.0 M NaClO$_4$ solution: Curve a: a fresh sputtered silver sample in air. Curve b: same sample in 1.0 M NaClO$_4$ solution at the open-circuit condition. Curve c: the sample used in b after being reduced at −0.15 V in 1.0 M NaClO$_4$ solution vs SSCE to collect −15.0 mC of charge. Curve d: the sample used in c after being partially reoxidized (Q_a = 25.0 mC) in 0.1 M NaOH and 0.9 M NaClO$_4$ solution. Curve e: an electrochemically grown silver oxide film (Q_a = 9.0 mC) in 0.1 M NaOH and 0.9 M NaClO$_4$ solution. Curve f: QCM frequency change for an oxidized sputtered antimicrobial silver sample in chloride media.

that some of the antimicrobial silver samples contain high percentages of both Ag(0) and Ag(I) species while the electrochemically grown silver oxide contains nearly 100% of Ag(I) species. To see whether a highly reduced antimicrobial silver film has an appreciable dissolution rate, the potential of the sample was scanned from its rest potential to −0.15 V vs SSCE, where the reducible silver species was converted to Ag^0. The amount of charge collected, Q_c, was ca. −15.0 mC. Curve c shows the weight change of the reduced sample as a function of time in the same solution. As can be seen, no significant change in the weight was observed in a 1-h period. However, if the reduced sample was partially reoxidized (Q_a = 25.0 mC) back to silver oxide in 0.1 M NaOH and 0.9 M NaClO$_4$, the dissolution rate of the sample monitored in 1.0 M NaClO$_4$ was substantially enhanced, as shown in curve d of Figure 15. These results are consistent with the fact that Ag(I) species have a substantially higher solubility in water than pure silver metal.[23] In curve f of Figure 15, we also show the deposition/dissolution behavior of an oxidized antimicrobial silver film on the addition of chloride ion. A significant decrease in the frequency, other than that associated with the interference from movement caused by the introduction of solution, was observed when a 0.05 M NaCl solution was introduced into the cell. The introduction of an additional 0.05 M NaCl solution caused a further decrease in the frequency. These frequency decreases are interpreted as the weight gain when silver oxide is converted to the less soluble and heavier silver chloride. However, when an additional 1 M NaCl solution was introduced into the QCM cell, the QCM frequency started to increase (rather than decrease) with time, indicating a continuous loss in mass. The observed mass loss can probably be attributed to the formation of soluble chlorosilver(I) complexes, e.g., AgCl$_2^-$. Very similar deposition/dissolution behavior was also observed on an electrochemically grown silver oxide film (see Supporting Information). Finally, we should note that the initial dissolution of either electrochemically grown silver oxide or sputtered silver films in these solutions is predominantly a diffusion-controlled process, as manifested by the well-known square-root of time dependence of the mass loss.

Conclusions

The electrochemical results suggest that the antimicrobial films contain Ag(0) and Ag(I) in different proportions, the form of Ag(I) being Ag$_2$O, AgOH, or mixtures of these. While the

dissolution of metallic Ag or antimicrobial films totally converted to the Ag(0) form is small in aqueous 1.0 M NaClO$_4$ solution, films containing Ag(I) are soluble. The SECM results, e.g., the oxidation current observed at a tip above an antimicrobial film in the region where Ag(0) is known to oxidize, indicates that the dissolved silver species contains both Ag(I) and Ag(0). While the SECM measurements cannot provide structural information about this species, small clusters containing Ag(0) and Ag(I) (and O and H) are reasonable possibilities. Preliminary spectroscopic (optical and mass) studies, which will be reported elsewhere, seem to indicate that small silver/oxide clusters are present in the solution.

Supporting Information Available: More detailed information for the calibration of the QCM and some XRD data. This material is available free of charge via the Internet at http://pubs.acs.org.

References and Notes

(1) (a) See, e.g.: Hill, W. R.; Pillsbury, D. M. *Argyria−The Pharmacology of Silver*; Williams and Wilkins: Baltimore, 1939. (b) See, e.g.: Thompson, N. R. In *Comprehensive Inorganic Chemistry*; Bailer, J. C., Eméleus, H. J., Nyholm, R., Trutman-Dickeson, A. F., Eds.; Pergamon Press: Oxford, U.K., 1973; Vol. IIID.

(2) Gibbard, J. *J. Am. Public Health* **1937**, *27,* 122.

(3) Fox, C. *Int. Surg.* **1975**, *60,* 275.

(4) Newell, F. *Am. J. Ophthalmol.* **1980**, *90,* 874.

(5) Spadaro, J. A. In *Moderm Bioelectricity*; Marino, A. A.*,* Ed.; Marcel Dekker: New York, 1988.

(6) Acél, D. Z. *Biochemistry* **1920**, *112,* 23.

(7) Djokic, S. S.; Burrell, R. E. *J. Electrochem. Soc.* **1998**, *145,* 1426.

(8) Olson, M. E.; Wright, J. B.; Burrell, R. E. *Eur. J. Surg.* **2000**, *166,* 486.

(9) Fan, F.-R.; Bard, A. J. *J. Electrochem. Soc.* **1989**, *136,* 3216.

(10) (a) Bard, A. J.; Fan, F.-R.; Mirkin, M. V. In *Electroanalytical Chemistry*; Bard, A. J., Ed.; Marcel Dekker: New York, 1994; Vol. 18, pp 243−373. (b) Bard, A. J.; Mirkin, M. V., Eds. *Scanning Electrochemical Microscopy*; Marcel Dekker: New York, 2001.

(11) Cliffel, D. E.; Bard, A. J. *Anal. Chem.* **1998**, *70,* 1993.

(12) Martin, B. A.; Hager, H. E. *J. Appl. Phys.* **1989**, *65,* 2627.

(13) Bard, A. J.; Faulkner, L. R. *Electrochemical Methods: Fundamentals and Applications*, 2nd ed.; J. Wiley & Sons: New York, 2001.

(14) (a) Shumilova, N. A.; Zhutaeva, G. V. In *Encyclopedia of Electrochemistry of The Elements*; Bard, A. J., Ed.; Marcel Dekker: New York, 1978; Vol. VIII. (b) Dirkse, T. P. *Electrochim. Acta* **1990**, *36,* 1445.

(15) Bard, A. J.; Denuault, G.; Friesner, R. A.; Dornblaser, B. C.; Tuckerman, L. S. *Anal. Chem.* **1991**, *63,* 1282.

(16) (a) Oglesby, D. M.; Omang, S. H.; Reilley, C. N. *Anal. Chem.* **1965**, *37,* 1312. (b) Hubbard, A. T.; Anson, F. C. In *Electroanalytical Chemistry*; Bard, A. J., Ed.; Marcel Dekker: New York, 1970; Vol. 4, pp 129−213.

(17) (a) Meites, L. *J. Am. Chem. Soc.* **1951**, *73*, 395. Meites, L. *J. Am. Chem. Soc.* **1951**, *73,* 1581. (b) West, P. W.; Dean, J.; Breda, E. J. *Collect. Czech. Chem. Commun.* **1948**, *13,* 1.

(18) ten Kortenaar, M. V.; Kolar, Z. I.; Tichelaar, F. D. *J. Phys. Chem. B* **1999**, *103,* 2054.

(19) (a) Henglein, A. *J. Phys. Chem.* **1993**, *97,* 5457. (b) Mostafavi, M.; Keghouche, N.; Belloni, J. *Chem. Phys. Lett.* **1990**, *167,* 193. (c) Linnert, T.; Mulvaney, P.; Henglein, A.; Weller, H. *J. Am. Chem. Soc.* **1990**, *112,* 4657.

(20) (a) Peyser, L. A.; Vinson, A. E.; Bartko, A. P.; Dickson, R. M. *Science* **2001**, *291,* 103. (b) Devore, T. C.; Woodward, J. R.; Le, P. N.; Gole, J. L.; Dixon, D. A. *J. Phys. Chem.* **1990**, *94,* 756.

(21) Kautek, W.; Dieluweit, S.; Sahre, M. *J. Phys. Chem.* **1997**, *101,* 2709.

(22) (a) Dirkse, T. P.; De Vries, D. B. *J. Phys. Chem.* **1959**, *63,* 107. (b) Nagy, G. D.; Casey, E. J. In *Zinc−Silver Oxide Batteries*; Fleischer, A.; Lander, J. J., Eds.; The Electrochemical Society Series; John Wiley & Sons: New York, 1971; pp 133−151.

(23) Linke, W. F. *Solubilities, Inorganic and Metal Organic Compounds*, 4th ed.; American Chemical Society: Washington, DC, 1965.